1-2014

Aerosol single scattering albedo dependence on biomass combustion efficiency: Laboratory and field studies

Shang Liu
Los Alamos National Laboratory

Allison C. Aiken
Los Alamos National Laboratory

Caleb Arata
Los Alamos National Laboratory

Manvendra K. Dubey
Los Alamos National Laboratory

C. Stockwell
University of Montana - Missoula

See next page for additional authors

Recommended Citation

Authors

Shang Liu, Allison C. Aiken, Caleb Arata, Manvendra K. Dubey, C. Stockwell, Robert Yokelson, Elizabeth A. Stone, Thilina Jayarathne, Allen L. Robinson, Paul J. DeMott, and Sonia M. Kreidenweis

RESEARCH ARTICLE

Aerosol single scattering albedo dependence on biomass combustion efficiency: Laboratory and field studies

Shang Liu[1], Allison C. Aiken[1], Caleb Arata[1], Manvendra K. Dubey[1], Chelsea E. Stockwell[2], Robert J. Yokelson[2], Elizabeth A. Stone[3], Thilina Jayarathne[3], Allen L. Robinson[4], Paul J. DeMott[5], and Sonia M. Kreidenweis[5]

[1]Earth and Environmental Sciences Division, Los Alamos National Laboratory, Los Alamos, New Mexico, USA, [2]Department of Chemistry, University of Montana, Missoula, Montana, USA, [3]Department of Chemistry, University of Iowa, Iowa City, Iowa, USA, [4]Center for Atmospheric Particle Studies, Carnegie Mellon University, Pittsburgh, Pennsylvania, USA, [5]Department of Atmospheric Science, Colorado State University, Fort Collins, Colorado, USA

Abstract Single scattering albedo (ω) of fresh biomass burning (BB) aerosols produced from 92 controlled laboratory combustion experiments of 20 different woods and grasses was analyzed to determine the factors that control the variability in ω. Results show that ω varies strongly with fire-integrated modified combustion efficiency (MCE$_{FI}$)—higher MCE$_{FI}$ results in lower ω values and greater spectral dependence of ω. A parameterization of ω as a function of MCE$_{FI}$ for fresh BB aerosols is derived from the laboratory data and is evaluated by field observations from two wildfires. The parameterization suggests that MCE$_{FI}$ explains 60% of the variability in ω, while the 40% unexplained variability could be accounted for by other parameters such as fuel type. Our parameterization provides a promising framework that requires further validation and is amenable for refinements to predict ω with greater confidence, which is critical for estimating the radiative forcing of BB aerosols.

1. Introduction

Biomass burning (BB) is one of the largest sources of carbonaceous aerosols that are known to affect the radiative balance of the Earth [*Bond et al.*, 2013]. The net BB radiative forcing is small ($0.0 \pm 0.20\,\mathrm{W\,m^{-2}}$) [*Intergovernmental Panel on Climate Change*, 2013] but very uncertain due to the need to resolve the balance between the positive forcing by black and brown carbon (BC, BrC) and the negative forcing by organic carbon (OC). Furthermore, since BB could increase as future warming accentuates favorable conditions for wildfires, it is important to quantify the magnitude and sign of this feedback.

Single scattering albedo (ω) is the key optical parameter that describes the magnitude and sign of aerosol's direct radiative forcing [*Ramanathan et al.*, 2001]. Consequently, the uncertainty in ω is the dominant source of uncertainty in the modeled direct aerosol radiative forcing, especially for the all-sky scenario simulation when clouds are present [*McComiskey et al.*, 2008]. In radiative-transfer modeling, the ω values are usually based on data from limited field measurements [*Chand et al.*, 2009], retrieved from inversion of radiometric measurements [*Sena et al.*, 2013] or modeled using the Mie theory with assumed refractive indices [*Chung and Seinfeld*, 2002]. It has been shown that the estimated ω values using these methods are inconsistent with each other [*Russell et al.*, 2002], which can cause a large bias in the model predictions, given the high sensitivity of the modeled forcing to ω [*Chung et al.*, 2012]. Moreover, one wavelength independent ω value is often assumed across the spectrum as model inputs, which can result in errors induced by the wavelength dependence of ω largely due to BrC and OC that has not been measured extensively. Therefore, more systematic optical measurements of BB aerosols that cover the range of atmospheric conditions and process-based parameterizations of fire emissions are urgently needed to constrain the model inputs and to reduce the uncertainties in prediction.

In this study, we conduct controlled laboratory combustion experiments using a range of globally significant fuels to explore the factors that control the variability of ω. We use our laboratory results to derive parameterizations to predict ω for fresh emissions that are then evaluated using field measurements. We assess the uncertainties and possible future refinements of the parameterization for its potential applications. The spectral dependence of ω and absorption for BB aerosols are also discussed.

2. Sampling Sites and Measurements

In this section, we describe the laboratory studies, field measurements, and the key instruments. More detailed information is presented in the supporting information.

2.1. Laboratory Measurements

The laboratory measurements were conducted in the U.S. Forest Service's Fire Science Laboratory in October and November of 2012 during the fourth Fire Laboratory at Missoula Experiment (FLAME-4). The laboratory combustion simulates open wildfires and cookstove fires with a wide range of globally important fuels, e.g., African grass, Canadian and Indonesian peat, rice straw from mainland China and Taiwan, and a variety of plants from across the United States (Table S1 in the supporting information). Altogether, BB aerosols of 20 types of fuels with 92 individual burns sampled from the exhaust stack (refers to "stack" burns) were studied in this work.

2.2. Wildfire Measurements

Ground-based field measurements of the Las Conchas (LC) and Whitewater Baldy (WB) wildfire emissions in New Mexico (U.S.) were performed during 7–15 July 2011 and 25 May to 13 June 2012, respectively. The sampling site was ~16 km east of where LC wildfire started and ~350 km northeast of the WB wildfire region. Therefore, the measured LC and WB fire plumes represent relatively fresh and aged (~9 h) BB aerosols, respectively. The similarity in the biomass types and their distributions in LC and WB regions enables direct comparison of the optical properties for fresh and aged BB aerosols. Flight measurements of the Lake McKay (LM) wildfire plumes (56.5°N, 106.8°W) were conducted on 1 July 2008 on the NASA DC8 aircraft during the Arctic Research of the Composition of the Troposphere from Aircraft and Satellites (ARCTAS) project. Fresh LM fire plumes with aging time less than 4 h were sampled.

2.3. Methods

During FLAME-4 and LC and WB wildfire measurements, the absorption (b_{abs}^{λ}) and scattering (b_{scat}^{λ}) coefficients at 405 nm, 532 nm, and 781 nm were measured using a three-wavelength photoacoustic soot spectrometer (Droplet Measurement Technologies, Inc., CO) at relative humidity < 30% [*Flowers et al.*, 2010]. For the LM wildfire measurement, b_{scat}^{532} and b_{abs}^{532} for submicron particles were measured by a nephelometer (Radiance Research, Seattle, WA, USA) and a Radiance Research three-wavelength particle soot absorption photometer (PSAP), respectively. The nephelometer data were corrected for truncation errors [*Anderson and Ogren*, 1998], and the PSAP data were corrected following the method of *Virkkula* [2010], which was derived based on comparing the performance of the PSAP with the photoacoustic method. The laboratory fire-integrated ω values were calculated as the ratio of fire-integrated scattering to fire-integrated extinction, using total summed values of scattering and extinction that implicitly account for varying masses of emissions across all burn phases.

The mixing ratios of CO and CO_2 were measured simultaneously by an open path Fourier transform infrared spectrometer system during FLAME-4 [*Burling et al.*, 2010]. The fire-integrated modified combustion efficiency (MCE_{FI}) is quantified as $\Delta[CO_2]/(\Delta[CO_2] + \Delta[CO])$ [*Yokelson et al.*, 2008], where ΔCO and ΔCO_2 represent fire-integrated excess CO and CO_2 mixing ratios during a burn, respectively. The background CO and CO_2 mixing ratios were the CO and CO_2 mixing ratios right before the ignition of each burn. Gas phase measurements during WB and LM wildfires are described in the supporting information.

During FLAME-4, the mass of particulate elemental carbon (EC) and OC in BB aerosols was quantified using quartz filter samples that were analyzed with a Sunset EC-OC aerosol analyzer (Sunset Laboratory, Forest Grove, USA). The split of EC and OC was determined using the filter optical transmittance. The EC and OC data are used qualitatively only in this work, i.e., EC is used as a surrogate for BC, and the ratio of OC to EC is used to qualitatively indicate the relative magnitude of OC and BC.

3. Results and Discussion

3.1. Dependence of ω on Combustion Efficiency From FLAME-4

The ω values of BB aerosols during FLAME-4 span a large range of ~0.2–1 (Table S1) and exhibit a strong dependence on MCE_{FI} (Figures 1a–1c). Similar patterns of ω versus MCE_{FI} of different fuels are observed. The
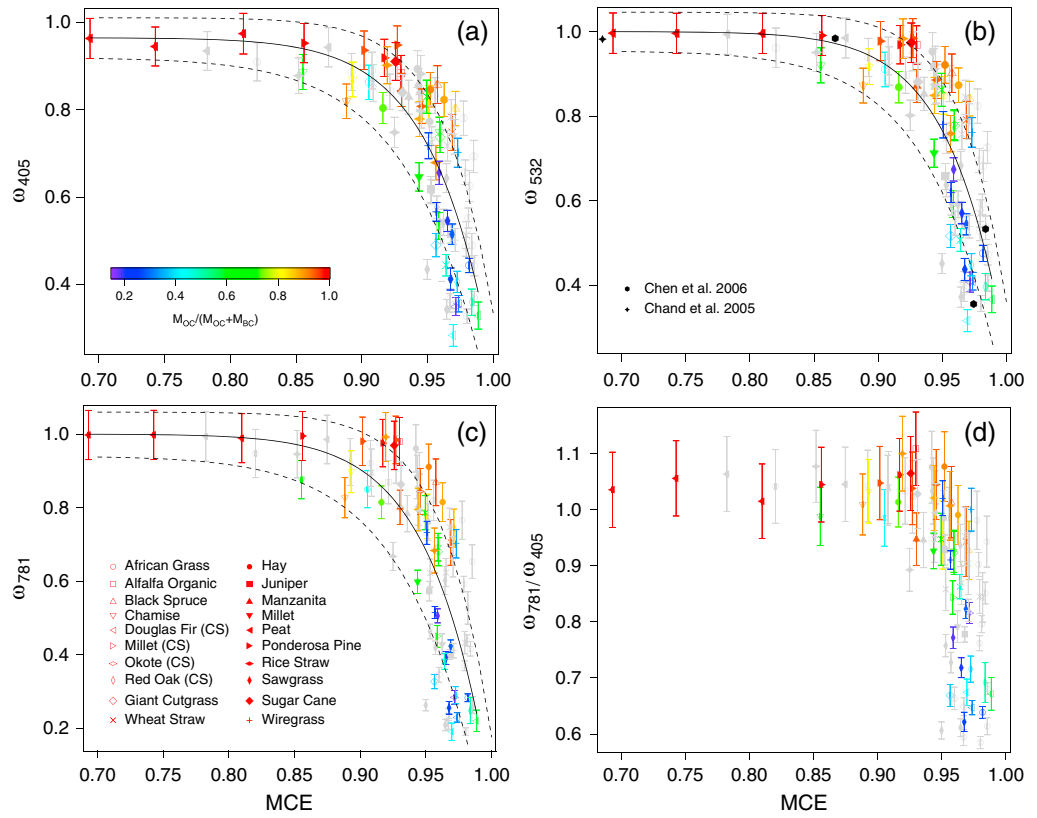
Figure 1. Fire-integrated ω as a function of fire-integrated MCE at (a) 405 nm, (b) 532 nm, and (c) 781 nm measured during FLAME-4. The solid and dashed lines represent the best fit and the uncertainty bounds (calculated using the fitting errors in Table 1), respectively. (d) The ratio of ω_{781} to ω_{405} versus MCE$_{FI}$. The symbols of the points represent fuel types listed in the legend, in which "CS" indicates cookstove studies. The points are colored by the ratio of OC mass (M_{OC}) to the total mass of OC and BC ($M_{OC} + M_{BC}$). The grey points indicate experiments with no EC-OC data. The error bars are calculated using 5% and 10% relative uncertainty in the b_{abs} and b_{scat} measurements, respectively. Measurements from *Chen et al.* [2006] and *Chand et al.* [2005] (Figure 1b). Note that the point of Chand et al. represents ω_{540} and MCE range of 0.02–0.56 in their measurements.

dependence of ω on MCE$_{FI}$ can be explained by the variation in chemical composition of BB aerosols produced under different combustion conditions. Specifically, because BC is generated by flaming combustion while OC is primarily produced by smoldering combustion [*McMeeking et al.*, 2009], the mass fraction of OC (out of the sum of OC and BC) decreases from ~80% to ~20% as MCE$_{FI}$ increases from ~0.85 to ~1 in our observations, a trend that is consistent with previous findings [*Christian et al.*, 2003]. The large decrease of OC relative to BC for MCE$_{FI} > 0.85$ measurements results in a sharp decrease of ω in the relatively high MCE combustions. Aerosols emitted from the low MCE combustion (MCE$_{FI} < 0.85$) are dominated by OC, resulting in high ω (~0.95) with small variability. In addition, the strong dependence of ω on MCE$_{FI}$ explains the large variation of ω for the repeated burns of the same fuels. For example, the African grass combustion aerosols exhibit ω_{532} (ω at 532 nm) of 0.36–0.96 that decreases with MCE$_{FI}$ (Table S1). Moreover, the ω versus MCE$_{FI}$ trend from FLAME-4 compares well with previous laboratory studies [*Chand et al.*, 2005; *Chen et al.*, 2006] (Figure 1b) but dramatically increases the coverage of MCE and ω and extends to multiple wavelengths, strengthening the repeatability of the laboratory measurements.

Table 1. Fitting Coefficients of ω as a Function of MCE$_{FI}$ ($y = k_0 + k_1 x^{k_2}$) and Coefficient of Determination (R^2) for the ω_{405}, ω_{532}, and ω_{781} Fits[a]

Wavelength (nm)	k_0	k_1	k_2	R^2
405	0.965 (±0.046)	−0.747 (±0.071)	21.718 (±4.710)	0.60
532	1.000 (±0.046)	−0.762 (±0.077)	23.003 (±5.090)	0.60
781	1.000 (±0.060)	−0.978 (±0.095)	22.016 (±4.800)	0.61

[a]Numbers in the parentheses represent the standard errors of the fitting coefficients.
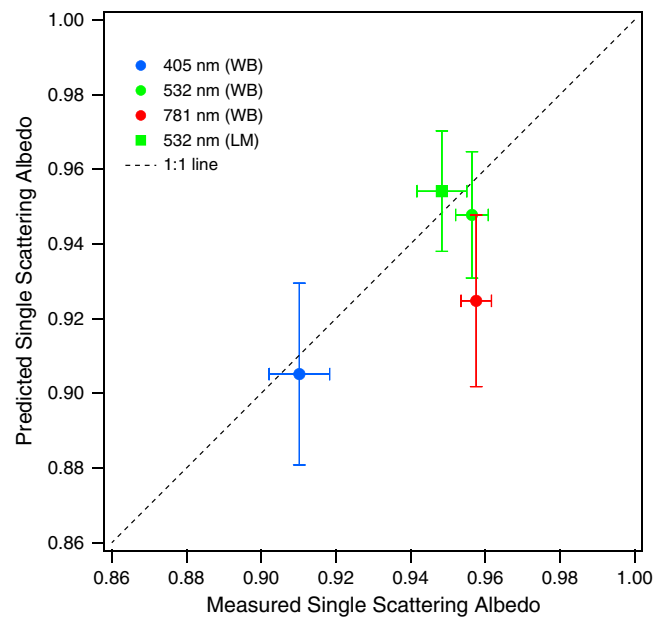
Figure 2. Predicted versus measured fire-integrated ω for the WB and LM fire plumes.

Since ω depends strongly on MCE_{FI}, which is measured more easily in the field, and can be estimated from archived emission factors of CO_2 and CO for a variety of BB types [*Akagi et al.*, 2011] or predicted in fire dynamics models [*Clark et al.*, 2010], it is desirable to derive quantitative dependence of ω on MCE_{FI}. In this work, we use the fire-integrated ω, which is typically used for wildfire emissions in climate models [*Chand et al.*, 2009], and the fire-integrated MCE to quantify their relationship. The cookstove burns are included in the fitting because the major difference between cookstove burns and open burns is that the former has improved combustion efficiency, and the combustion efficiency induced variation in ω should be captured in the fitting of ω as a function of MCE_{FI}. This is confirmed by the nearly identical fitting coefficients resulting from the fits with and without cookstove measurements. The power law function ($y = k_0 + k_1 x^{k_2}$) is used to fit the points in Figures 1a–1c with the constraint that ω is equal to or smaller than 1. The fitting coefficients, their standard errors, and the coefficient of determination (R^2) values for ω_{405}, ω_{532}, and ω_{781} are listed in Table 1.

3.2. Evaluation of Parameterization With Wildfire Emissions

The lab fire-based parameterization of ω as a function of MCE_{FI} is tested using the WB and LM wildfire measurements. The MCE_{FI} of the WB wildfire is estimated using the CO_2 and CH_4 measurements, since CO data were absent. The basis of using CH_4 instead of CO is that both CH_4 and CO are predominantly emitted from smoldering combustion, so correlation of CH_4 and CO is expected [*McMeeking et al.*, 2009]. A linear relationship of MCE_{FI} and the ratio of $EFCO_2$ (emission factor of CO_2) to $EFCH_4$ (emission factor of CH_4) are found from the FLAME-4 measurement and used to estimate MCE_{FI} for the WB wildfire (supporting information).

The predicted fire-integrated ω values using the fitting coefficients (Table 1) are compared with the measured fire-integrated ω values at 405 nm, 532 nm, and 781 nm (Figure 2). Good agreement is achieved. For the WB wildfire, the absolute and fractional differences between predicted and measured ω are [0.005, 0.009, 0.033] and [0.6%, 0.9%, 3.6%] for [ω_{405}, ω_{532}, ω_{781}], respectively. Relatively larger deviation is observed at 781 nm. Additional comparisons using future field measurements are needed to verify and explain this behavior. The lower predicted ω can result from (1) the uncertainties in the MCE_{FI} calculation during the WB wildfire, i.e., using CH_4 instead of CO to estimate MCE_{FI}, (2) the WB wildfire aerosols are aged for ~9 h so ω may increase, while the fitting coefficients are derived for fresh BB emissions, and (3) fitting uncertainty. For the LM wildfire, the absolute and fractional differences between predicted and measured ω_{532} are 0.006 and 0.6%, respectively.
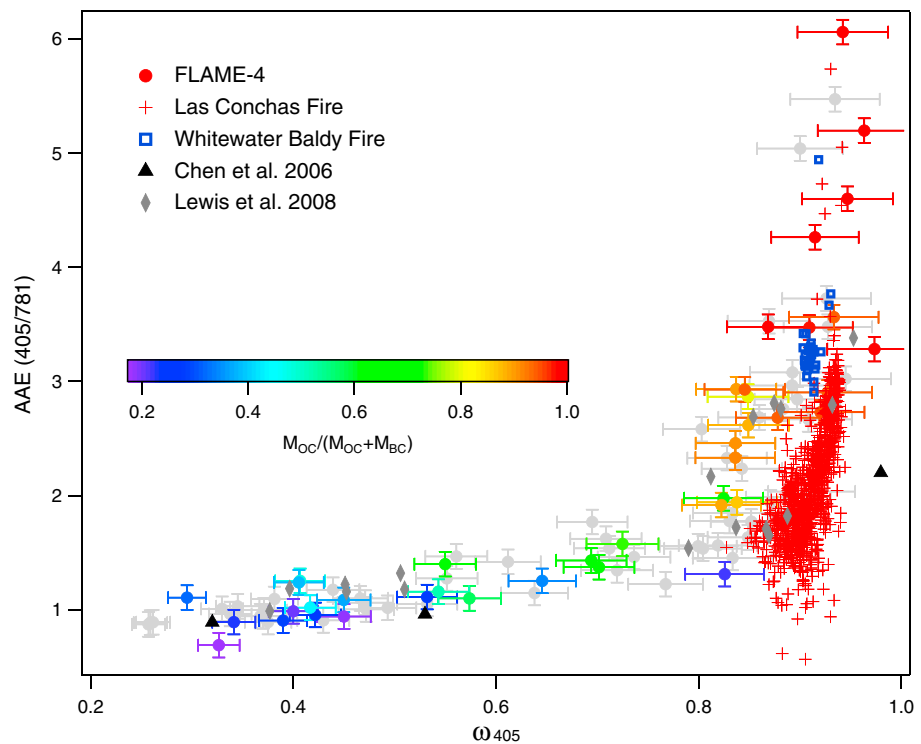
Figure 3. Fire-integrated $AAE_{405nm/781nm}$ versus ω_{405} during FLAME-4 overlaid with LC wildfire, WB wildfire, and earlier laboratory measurements. Each of the FLAME-4 burns is colored by the mass fraction of OC to the total mass of OC and BC. The LC and WB wildfire measurements are 5 min averages of the fire plumes. Note the points of *Lewis et al.* [2008] represent $AAE_{405nm/870nm}$ and ω_{405}, and the points of *Chen et al.* [2006] represent $AAE_{532nm/1047nm}$ and ω_{532}.

3.3. Parameterization Uncertainty, Application, and Refinement

The R^2 values of the fits (Table 1) suggest that MCE_{FI} explains 60% of the observed variability in ω, indicating that the selected fitting function (of the ~15 explored) captures the systematic trends over the large range of ω and MCE investigated in our laboratory study. The unexplained variation in ω that amounts to 40% could be driven by other parameters such as fuel type, which are not resolved and could reduce the accuracy of model prediction using the derived fitting coefficients. In addition, the increase of ω with photochemical aging could limit the application of the parameterization to fresh wildfire emissions if the change is significant. We note that for the ~9 h old WB wildfire our parameterization performed well. Furthermore, limited MCE data from wildfires tend to be lower than the laboratory measured MCE due to the ideal conditions in the laboratory [*Christian et al.*, 2003], suggesting an MCE-induced uncertainty; thus, the MCE from field data should be used for predicting ω for each ecosystem. Further wildfire observations of both ω and MCE should be prioritized to evaluate and refine our parameterization.

Although uncertainties are expected, our parameterization does capture the gross mechanistic features and the average behavior of real wildfires. Since mixed fuels are burned during wildfires, the positive and negative uncertainties in the parameterization (Figures 1a–1c) may offset each other. Therefore, the overall uncertainty of our parameterization for wildfires is likely smaller than the uncertainty estimated from laboratory burns with single species. The good comparison of the predicted and measured ω for wildfires (section 3.2) provides evidence for this, but measurements with more fires are needed to refine this further. We recommend that the parameterization could be used with the aforementioned caveats by modelers. Moreover, our parameterization is valuable for sensitivity studies using nested grid Weather Research Forecast model that resolves fires to evaluate fire-climate feedback. For example, the fitting curves suggest that a small perturbation in MCE_{FI} [*Akagi et al.*, 2011] can lead to a large variation of ω for the BB aerosols. An increase of MCE_{FI} from 0.950 to 0.965 results in a decrease of 0.10 in ω_{532}, which could reduce the aerosol-induced change in upwelling flux at the top of the atmosphere by 50% and 100% over dark and bright surfaces, respectively [*Russell et al.*, 2002]. Overall, our parameterization explains a large fraction of the variation in ω and can serve

as a framework for predicting ω. The parameterization can be refined further by future measurements of mixed types of fuels in laboratory combustion and more extensive wildfire observations. Furthermore, a better understanding of the variation in ω with photochemical aging, specifically clarifying if this change occurs on the flat or steep side of our ω versus MCE_{FI} parameterization, should enhance its predictive power and applicability to wildfires.

3.4. Spectral Dependence of Aerosol Absorption and Single Scattering Albedo

Figure 3 illustrates absorption Ångström exponent (AAE) as a function of ω_{405}. The AAE increases sharply from ~2 to ~6 with ω increasing from ~0.8 to ~1 (OC mass fraction larger than 80%), confirming that a large amount of light-absorbing organic carbon (brown carbon, BrC) is emitted during low MCE combustion that enhances the wavelength dependence of BB aerosols [*Kirchstetter et al.*, 2004]. Compared with previous laboratory studies [*Lewis et al.*, 2008; *Chen et al.*, 2006], the AAE versus ω pattern in Figure 3 shows a more distinct trend due to the larger range of fuel types and number of burns sampled during FLAME-4 that yield better statistics.

The average ω values of the LC and WB wildfires are comparable, with the values of 0.908 and 0.911, respectively, but statistical test shows that the ω of the aged WB wildfire is significantly larger than the ω of the fresh LC wildfire at 95% confidence level (*t* test $P = 0.02$) because of the larger variability in ω during the LC wildfire measurements. This is consistent with the results of *Yokelson et al.* [2009] that shows increasing ω during atmospheric aging due to the increasing OC mass fraction. Furthermore, the variability in ω of the WB wildfire (0.90–0.93) is significantly smaller than that in the LC wildfire (0.83–0.95). Part of the lower variability of WB ω could arise from the WB fire plume being sampled over a shorter period than the LC fire; however, the smaller variability in ω of aged BB aerosols suggests that the aged BB aerosols can have more uniform optical properties, reflecting the possible convergence of aerosol chemical composition with atmospheric oxidation [*Hennigan et al.*, 2011] and increased internal mixing. In addition, the AAE of the aged BB aerosols, 3.3 ± 0.4 (1σ), is significantly higher than the AAE of the fresh BB aerosols, 2.1 ± 0.5 (1σ), consistent with a recent smog chamber study showing an increasing AAE with aging of BB aerosols [*Saleh et al.*, 2013]. The higher AAE of aged BB aerosols supports the secondary formation of BrC in the atmosphere that has been confirmed in laboratory studies [*Chang and Thompson*, 2010].

The wavelength dependence of ω is observed during FLAME-4 (Figure 1d). Since ω is determined by the ratio of scattering to absorption, the spectral dependence of ω depends on the relative spectral dependence of scattering (quantified by scattering Ångström exponent, SAE) and absorption, i.e., the difference between SAE and AAE. In other words, larger differences between SAE and AAE result in greater spectral dependence of ω. Values of ω_{405} and ω_{532} are not significantly different (*t* test $P = 0.14$), while ω_{781} is significantly smaller (on average 13%) than ω_{532} at 95% confidence level (*t* test $P = 0.01$). This is due to the observation that the scattering coefficient has stronger wavelength dependence than the absorption coefficient, i.e., SAE > AAE for high MCE_{FI} measurements [*Bergstrom et al.*, 2003]. The wavelength dependence of ω is weaker at lower MCE_{FI} values (Figure 1d), likely because of the emission of BrC during the low-efficiency combustion that significantly enhances the AAE, thereby reducing the difference between the SAE and AAE. The large spectral variation of ω at high MCE_{FI} underscores the need to estimate ω at multiple wavelengths for radiative forcing calculations.

4. Conclusion

We demonstrated that although ω of BB aerosols spans a large range (~0.2–1) and shows strong spectral dependence, 60% of its variation can be explained and captured by MCE_{FI}, while the remaining unexplained variability could be due to fuel type or other parameters. A framework to predict ω as a function of MCE_{FI} has been established from laboratory fires and confirmed with two wildfire measurements. Since MCE_{FI} has been measured extensively for most major vegetation classes and types of biomass burning [*Akagi et al.*, 2011], our reported parameterization could be used to predict the ω of fresh smoke for most fire types to estimate their radiative forcing in climate models with additional verification and refinement being desirable. Our model predicted the ~9 h old aged WB fire plume well. However, we note that further wildfire measurements, particularly at lower ω values, are needed to verify and refine the parameterization. In addition, our results show that both ω and AAE increase with aging, so if aging effects on ω are also modeled [*Yokelson et al.*, 2009], this

could further improve the radiative forcing estimates for BB and allow enhanced modeling of coupled climate-fire feedback. This work reinforces the importance of evaluating aerosol ω under different combustion conditions as well as at multiple wavelengths, both of which could potentially enhance the accuracy in the predicted radiative forcing of BB aerosols.

References

Akagi, S., R. Yokelson, C. Wiedinmyer, M. Alvarado, J. Reid, T. Karl, J. Crounse, and P. Wennberg (2011), Emission factors for open and domestic biomass burning for use in atmospheric models, *Atmos. Chem. Phys.*, *11*(9), 4039–4072.

Anderson, T. L., and J. A. Ogren (1998), Determining aerosol radiative properties using the TSI 3563 integrating nephelometer, *Aerosol Sci. Technol.*, *29*(1), 57–69.

Bergstrom, R. W., P. Pilewskie, B. Schmid, and P. B. Russell (2003), Estimates of the spectral aerosol single scattering albedo and aerosol radiative effects during SAFARI 2000, *J. Geophys. Res.*, *108*(D13), 8474, doi:10.1029/2002JD002435.

Bond, T., et al. (2013), Bounding the role of black carbon in the climate system: A scientific assessment, *J. Geophys. Res. Atmos.*, *118*, 5380–5552, doi:10.1002/jgrd.50171.

Burling, I., R. J. Yokelson, D. W. Griffith, T. J. Johnson, P. Veres, J. Roberts, C. Warneke, S. Urbanski, J. Reardon, and D. Weise (2010), Laboratory measurements of trace gas emissions from biomass burning of fuel types from the southeastern and southwestern United States, *Atmos. Chem. Phys.*, *10*(22), 11,115–11,130.

Chand, D., O. Schmid, P. Gwaze, R. Parmar, G. Helas, K. Zeromskiene, A. Wiedensohler, A. Massling, and M. Andreae (2005), Laboratory measurements of smoke optical properties from the burning of Indonesian peat and other types of biomass, *Geophys. Res. Lett.*, *32*, L12819, doi:10.1029/2005GL022678.

Chand, D., R. Wood, T. Anderson, S. Satheesh, and R. Charlson (2009), Satellite-derived direct radiative effect of aerosols dependent on cloud cover, *Nat. Geosci.*, *2*(3), 181–184.

Chang, J. L., and J. E. Thompson (2010), Characterization of colored products formed during irradiation of aqueous solutions containing H_2O_2 and phenolic compounds, *Atmos. Environ.*, *44*(4), 541–551.

Chen, L. W. A., H. Moosmüller, W. P. Arnott, J. C. Chow, J. G. Watson, R. A. Susott, R. E. Babbitt, C. E. Wold, E. N. Lincoln, and W. M. Hao (2006), Particle emissions from laboratory combustion of wildland fuels: In situ optical and mass measurements, *Geophys. Res. Lett.*, *33*, L04803, doi:10.1029/2005GL024838.

Christian, T., B. Kleiss, R. Yokelson, R. Holzinger, P. Crutzen, W. Hao, B. Saharjo, and D. Ward (2003), Comprehensive laboratory measurements of biomass-burning emissions: 1. Emissions from Indonesian, African, and other fuels, *J. Geophys. Res.*, *108*(D23), 4719, doi:10.1029/2003JD003704.

Chung, C. E., V. Ramanathan, and D. Decremer (2012), Observationally constrained estimates of carbonaceous aerosol radiative forcing, *Proc. Natl. Acad. Sci. U.S.A.*, *109*(29), 11,624–11,629.

Chung, S. H., and J. H. Seinfeld (2002), Global distribution and climate forcing of carbonaceous aerosols, *J. Geophys. Res.*, *107*(D19), 4407, doi:10.1029/2001JD001397.

Clark, M. M., T. H. Fletcher, and R. R. Linn (2010), A sub-grid, mixture–fraction-based thermodynamic equilibrium model for gas phase combustion in FIRETEC: Development and results, *Int. J. Wildland Fire*, *19*(2), 202–212.

Flowers, B., M. Dubey, C. Mazzoleni, E. Stone, J. Schauer, S.-W. Kim, and S. Yoon (2010), Optical-chemical-microphysical relationships and closure studies for mixed carbonaceous aerosols observed at Jeju Island; 3-laser photoacoustic spectrometer, particle sizing, and filter analysis, *Atmos. Chem. Phys.*, *10*(21), 10,387–10,398.

Hennigan, C., M. Miracolo, G. Engelhart, A. May, A. Presto, T. Lee, A. Sullivan, G. McMeeking, H. Coe, and C. Wold (2011), Chemical and physical transformations of organic aerosol from the photo-oxidation of open biomass burning emissions in an environmental chamber, *Atmos. Chem. Phys.*, *11*(15), 7669–7686.

Intergovernmental Panel on Climate Change (2013), Anthropogenic and natural radiative forcing, in *Climate Change 2013: The Physical Science Basis*, chap. 8, p. 27, Cambridge Univ. Press, New York.

Kirchstetter, T. W., T. Novakov, and P. V. Hobbs (2004), Evidence that the spectral dependence of light absorption by aerosols is affected by organic carbon, *J. Geophys. Res.*, *109*, D21208, doi:10.1029/2004JD004999.

Lewis, K., W. P. Arnott, H. Moosmüller, and C. E. Wold (2008), Strong spectral variation of biomass smoke light absorption and single scattering albedo observed with a novel dual-wavelength photoacoustic instrument, *J. Geophys. Res.*, *113*, D16203, doi:10.1029/2007JD009699.

McComiskey, A., S. E. Schwartz, B. Schmid, H. Guan, E. R. Lewis, P. Ricchiazzi, and J. A. Ogren (2008), Direct aerosol forcing: Calculation from observables and sensitivities to inputs, *J. Geophys. Res.*, *113*, D09202, doi:10.1029/2007JD009170.

McMeeking, G. R., S. M. Kreidenweis, S. Baker, C. M. Carrico, J. C. Chow, J. L. Collett, W. M. Hao, A. S. Holden, T. W. Kirchstetter, and W. C. Malm (2009), Emissions of trace gases and aerosols during the open combustion of biomass in the laboratory, *J. Geophys. Res.*, *114*, D19210, doi:10.1029/2009JD011836.

Ramanathan, V., P. Crutzen, J. Kiehl, and D. Rosenfeld (2001), Aerosols, climate, and the hydrological cycle, *Science*, *294*(5549), 2119–2124.

Russell, P., J. Redemann, B. Schmid, R. Bergstrom, J. Livingston, D. McIntosh, S. Ramirez, S. Hartley, P. Hobbs, and P. Quinn (2002), Comparison of aerosol single scattering albedos derived by diverse techniques in two North Atlantic experiments, *J. Atmos. Sci.*, *59*(3), 609–619.

Saleh, R., C. Hennigan, G. McMeeking, W. Chuang, E. Robinson, H. Coe, N. Donahue, and A. Robinson (2013), Absorptivity of brown carbon in fresh and photo-chemically aged biomass-burning emissions, *Atmos. Chem. Phys.*, *13*, 7683–7693.

Sena, E., P. Artaxo, and A. Correia (2013), Spatial variability of the direct radiative forcing of biomass burning aerosols and the effects of land use change in Amazonia, *Atmos. Chem. Phys.*, *13*(3), 1261–1275.

Virkkula, A. (2010), Correction of the calibration of the 3-wavelength particle soot absorption photometer (3λ PSAP), *Aerosol Sci. Technol.*, *44*, 706–712.

Yokelson, R., T. Christian, T. Karl, and A. Guenther (2008), The tropical forest and fire emissions experiment: Laboratory fire measurements and synthesis of campaign data, *Atmos. Chem. Phys.*, *8*(13), 3509–3527.

Yokelson, R., J. Crounse, P. DeCarlo, T. Karl, S. Urbanski, E. Atlas, T. Campos, Y. Shinozuka, V. Kapustin, and A. Clarke (2009), Emissions from biomass burning in the Yucatan, *Atmos. Chem. Phys.*, *9*, 5785–5812.